EUROPEAN ORGANIZATION FOR NUCLEAR RESEARCH

CERN - PS DIVISION

CERN/PS 2000-063 (OP)

OPTIMISATION OF A MAGNETIC QUADRUPOLE PICK-UP STRUCTURE USING HFSS

A. Jansson *

Abstract

A magnetic quadrupole pick-up has recently been designed for the CERN proton synchrotron. The design is based on a new idea, where the undesired common mode signal is suppressed by coupling to the radial component of the field. One design detail is a thin resistive layer between the beam and the actual pick-up structure. This layer serves to lower the longitudinal impedance, but also influences the coupling impedance of the pick-up. To optimise the design, a series of simulations of the pick-up structure have been performed using the HFSS program. The longitudinal impedance was determined by simulating the coaxial wire-method, and the pick-up coupling to the different field modes created by the "beam" was studied and optimised. In this paper, the simulations are presented together with some comparative measurements.

* *Manne Siegbahn Laboratory/Stockholm University, Stockholm, Sweden*

ICAP 2000 Conference, 10-14 September 2000, Darmstadt, Germany

Geneva, Switzerland
30 November 2000

Optimisation of a magnetic quadrupole pick-up structure using HFSS

A. Jansson[†]

CERN, Geneva, Switzerland and
Manne Siegbahn Laboratory/Stockholm University, Stockholm, Sweden

(Dated: October 4, 2000)

A magnetic quadrupole pick-up has recently been designed for the CERN proton synchrotron. The design is based on a new idea, where the undesired common mode signal is suppressed by coupling to the radial component of the field. One design detail is a thin resistive layer between the beam and the actual pick-up structure. This layer serves to lower the longitudinal impedance, but also influences the coupling impedance of the pick-up. To optimise the design, a series of simulations of the pick-up structure have been performed using the HFSS program. The longitudinal impedance was determined by simulating the coaxial wire-method, and the pick-up coupling to the different field modes created by the "beam" was studied and optimised. In this paper, the simulations are presented together with some comparative measurements.

I. INTRODUCTION

A Quadrupole pick-ups

A quadrupole pick-up is an extension of the principle of a standard position pick-up. Just as a position pick-up measures the centre-of-mass (first moment) of a beam by probing the dipole field component it induces inside the beam pipe, a quadrupole pick-up measures the quadrupole moment $m_{\mathrm{Q}} = \sigma_{\mathrm{x}}^2 - \sigma_{\mathrm{y}}^2$ by means of the induced quadrupole field. The quadrupole moment is of interest since it contains information on the transverse beam sizes. This makes quadrupole pick-ups very interesting instruments for, for example, injection matching measurements, since they are non-invasive.

A common problem related to this type of pick-up is that the quadrupole signal is very small and embedded in a huge common-mode background. To solve this problem, a new design has been proposed where the common mode signal is inherently suppressed due to the special geometry of the pick-up[1]. The basic idea is to measure the radial component of the magnetic field, since it does not contain any common mode component. Although the principle of the design can be demonstrated analytically for simple geometries, bench measurements and simulations have been performed to understand and optimise the design details. This paper focuses mainly on the simulations.

[†]Andreas.Jansson@cern.ch

B The HFSS program

The High Frequency Structure Simulator[2] (HFSS) program simulates the electro-magnetic properties of structures using the Finite Element Method (FEM). It has a graphical user interface very similar to a CAD program, where a model of the structure can be drawn and a number of ports specified. The program then calculates the scattering parameters for the N-port in a chosen frequency range.

The simulation process has two main stages. First, the finite element mesh is created and optimised, and then a frequency sweep can be performed to study the frequency dependence of the s-parameters. The initial tetrahedra mesh is created using the available vertices in the model. It is very coarse and has to be refined in order to achieve an accurate result. A so-called adaptive mesh refinement is therefore performed. The mesh is refined by iteratively solving the problem and splitting the tetrahedra containing the highest field energy into smaller ones. This procedure makes sure that the mesh is only refined in areas where it is needed. In order for the adaptive refinement to work, the initial mesh has to be reasonably good, so that the power distribution is approximately correct. That means, generally, that the initial tetrahedra should not have too large aspect ratios (ratio between longest and shortest side), since the basic FEM approximation of interpolating the fields inside the tetrahedra from its values at the vertices then becomes invalid. The initial mesh can therefore be improved by adding extra vertices to the original model (seeding the mesh). The adaptive refinement is terminated when the changes in the simulated s-parameters between two iterations are below a pre-defined threshold.

The frequency sweep which follows can be performed in two ways. Either the problem is solved exactly for

each discrete point in the desired frequency range, or an approximate frequency dependence can be calculated from the solution at one given frequency. If the mesh is properly optimised and the frequency range reasonably narrow, the two methods give the same result. The approximate solution is however faster if many points within the range are to be calculated.

II. PICK-UP GEOMETRY AND MODELLING

A Basic mechanical design

The pick-up consists of four antenna loops wrapped around a ceramic vacuum chamber at 45° (see CAD drawing in Fig.1). Each loop covers an azimuthal angle of 45°, and measures the magnetic flux through it. The induced current in the loops is read out with current transformers. Two transformers are placed symmetrically around the ground point. The signals from these two transformers are then combined in a third transformer to a single output per loop. This arrangement gives a total load to each loop of the order of 0.1 Ω.

The ceramic chamber makes it possible to keep the loops outside the vacuum, thus avoiding cable feedtroughs and problems with vacuum compatibility of materials. To avoid build-up of static charges, the inside of the ceramic must be coated with a thin metallic layer. This layer also gives a certain screening effect at high frequencies, as discussed below.

The whole structure is enclosed in a copper casing resembling a pill-box cavity. This serves as by-pass for the wall current as well as a screen against outside noise. The dimensions of the structure are approximately 0.5 m (length) by 0.3 m (diameter).

B Modelling of the structure in HFSS

When modelling the pick-up in the HFSS program, the four-fold symmetry of the structure was used in order to reduce the problem size and save computing time. Thus, only one quadrant of the pick-up, containing a full antenna loop, was modelled. Wherever possible, metallic surfaces were assumed to be perfectly conducting, and thin objects were modelled as 2D sheets to obtain a stable initial mesh.

The transformer arrangement for the read-out of the loops was replaced by two ports with a characteristic impedance set to one half of the total loop load. Also, a port in each end of the vacuum chamber was provided to feed in the beam current. The model is shown in Fig.2.

Since HFSS cannot simulate particle beams, the beam was substituted by a thin wire. This is an approximation with limited validity, as discussed below, but the wire method is also the standard bench measurement method for the properties that were studied. Therefore, the simulations should compare well with reference measurements.

III. SIMULATION PROCEDURES

A Transfer impedance to pick-up outputs

The sensitivity of a pick-up is given by its transfer impedance. There is a different transfer impedance for each quantity to be measured (beam current, beam position etc.) Determination of the pick-up transfer impedances can be done by recording the response to an antenna wire at different transverse positions. A polynomial fit in antenna position then gives the sensitivity to beam current (constant term), beam position (linear term) and quadrupole moment (quadratic term). However, since the HFSS model only covers one fourth of the pick-up, image currents due to the symmetry planes also have to be accounted for. For the dipole field simulation, one H-type and one E-type boundary was introduced, with the H-type boundary running along the centre of the wire (see Fig. 3b). This is equivalent to two wires fed in anti-phase, and is thus a dipole antenna which simulates a beam offset. By varying the position of the wire relative to the E-type boundary, different beam positions can be simulated. For the quadrupole transfer impedance, the same setup was used, but with two H-type boundaries (see Fig. 3c). This is equivalent to two wires fed in-phase, which simulates a flat, centred beam. In the same way as above, different beam widths can be simulated by moving the wire. In both cases, the current in the "beam" wire will induce all possible field modes that are compatible with the symmetry boundaries. In the dipole field simulation, the strongest higher order mode is the sextupole field. In the case of the quadrupole field simulation, however, also the mono-pole mode is present since the total "beam" current is not zero. The effect of the different field modes must therefore be separated by polynomial fits, as described above.

B Longitudinal impedance seen by the beam

Any discontinuity in the beam pipe can upset the transverse nature of the electro-magnetic field and create a longitudinal voltage that acts back on the particles in the beam. The ratio between the induced longitudinal voltage and the beam current is called the longitudinal impedance. The longitudinal impedance of an object is usually measured with the coaxial wire method[3], in which a wire is stretched through the pick-up and the s_{21} parameter of the resulting coaxial transmission line is measured and compared to a reference vacuum pipe of the same length. Such a test-bench setup was simulated in HFSS. For this purpose, two H-type symmetry

boundaries were used, with the wire stretched along their intersection (see Fig. 3a).

For the conversion from s-parameters to longitudinal impedance there are several different formulae. If the object is much smaller than a wavelength, the lumped impedance approximation

$$Z = 2Z_c \frac{1 - \frac{s_{21,\mathrm{OBJ}}}{s_{21,\mathrm{REF}}}}{\frac{s_{21,\mathrm{OBJ}}}{s_{21,\mathrm{REF}}}} \tag{1}$$

can be used, where $s_{21,\mathrm{OBJ}}$ is the forward scattering parameter of the object under test, $s_{21,\mathrm{REF}}$ is the same parameter for a smooth pipe of the same length, and Z_c is the characteristic impedance of the coaxial line formed by the pipe and the wire. For homogeneously distributed impedances that are long compared to the wavelength, a better approximation is given by

$$Z = -2Z_c \ln \frac{s_{21,\mathrm{OBJ}}}{s_{21,\mathrm{REF}}}, \tag{2}$$

and f the electrical length $\theta = \omega \cdot l/c$ of the distributed impedance is known, an even better estimate can be obtained with[4]

$$Z = -2Z_c \ln \frac{s_{21,\mathrm{OBJ}}}{s_{21,\mathrm{REF}}} \left(1 + \mathrm{i}\, \frac{\ln \frac{s_{21,\mathrm{OBJ}}}{s_{21,\mathrm{REF}}}}{2\theta}\right). \tag{3}$$

All the above formulae are approximations valid for small impedances. The fact that there is not a unique formula illustrates a fundamental limitation with the coaxial wire method: it is not possible to determine the longitudinal impedance if the structure under test is considered as a 'black box'. The conversion of the s-parameter into an impedance is necessarily model-dependent, since the measured quantity is not directly the induced longitudinal voltage, but the attenuation and phase shift of the transmitted TEM-wave. For simple structures like the above cases of localised or homogeneously distributed impedances, this is not a problem, but for more complicated structures it can be hard to accurately interpret the s-parameter result, and one usually resorts to using one of the above formulae based on simple cases as approximation. It should, however, be noted that the Taylor expansions of the above formulae are all identical to first order in $\Delta s_{21} = s_{21,\mathrm{OBJ}} - s_{21,\mathrm{REF}}$. This condition coincides with the basic assumption in the derivation of these formulae: that the impedance should be small. Therefore, for small impedances ($Z << Z_c$) all three formulae give the same result. Likewise, for very large impedances ($Z >> Z_c$) all three formulae fail, and the choice of formula is therefore only important for intermediate impedances. Since the aim of the simulations presented here was not to establish an accurate value of large impedance peaks, but to find ways to suppress them, this limitation of the coaxial wire method was not considered a problem. Indeed, in the final version, the impedance of the pick-up was so small that all formulas gave approximately the same result. To be consistent, all the simulations presented here were interpreted using the log-formula in (2).

Another problem with the wire method is that the presence of the conducting wire changes the electromagnetic properties of the object being studied. Although the transverse field pattern from a round, centred, and ultra-relativistic beam inside a conducting pipe is identical to that of a TEM wave packet, the TEM wave can be reflected when it sees a local impedance, whereas the real beam can only excite non-propagating field modes at frequencies below the cut-off frequency of the beam pipe. Therefore, if several localised impedances are present, multiple reflections of the TEM-wave can occur, which show up as "false" impedance peaks at certain frequencies. Again, since the reflections are related to the magnitude of the longitudinal impedance, this problem is not so severe if one is mainly interested in minimising the impedance, rather than in determining its exact value.

C Meshing phase-lag problem and solution

The HFSS program allows for the addition or subtraction of a length l of matched transmission line to any port in the model, with subsequent re-calculation of the scattering parameters using the analytical formula

$$\tilde{s}_{21} = e^{\gamma l} \cdot s_{21} \tag{4}$$

where $\gamma = \alpha + j\beta$ is the propagation constant. This constant is calculated by the program from a 2D model of the port. Since the subtraction of a matched transmission line of the same length as the pick-up is equivalent to the division by the reference s-parameter in (2), this was initially used to obtain the quantity $s_{21,\mathrm{OBJ}}/s_{21,\mathrm{REF}}$.

It was found, however, that in the HFSS simulation result there was systematically a residual delay left after this correction, which turns into a non-physical reactive impedance. The delay is always positive (underestimates the phase) and increases linearly with frequency. The reason seems to be that the propagation constant calculated from the 2D model of the ports does not correspond to the simulated propagation of the wave through the 3D model. The effect decrease with increasing mesh size, as can be expected if the problem is related to the discretisation.

Since the mesh size is effectively limited by the computing resources, the problem was circumvented by simulating the reference s_{21}-parameter of the pipe only, using the same mesh but changing the material properties in the model to produce a smooth pipe without discontinuities (as seen from the inside).

IV. SIMULATION RESULTS

A Bare pick-up properties

As the pick-up measures the radial magnetic field, the loops must be situated a certain distance from the beam pipe, since otherwise its conducting boundary would prevent any magnetic flux through the loop. Since the antenna loops can not be moved closer to the beam, because they would then reduce the machine aperture, a local enlargement of the beam pipe is thus needed. This is the reason for the cavity. Figs. 4 and 5 show the simulated dependence of the transfer impedances on the radius of this cavity. The transfer impedances saturate for large radii, indicating that the presence of the conducting boundary is then no longer important. The quadrupole transfer impedance saturate faster since the quadrupole field falls of faster with the distance from the centre. Above saturation, no sensitivity is gained by increasing the radius. The value of the radius was set to 15 cm, above saturation for the quadrupole transfer impedance but slightly below for the dipole.

Another basic free parameter is the opening angle of the antenna loops. A larger angle would give more signal, but for too angles values inter-loop coupling might create problems, since the loops are then very close to each other. Figs. 6 and 7 show the simulated transfer impedances versus opening angle. The dipole transfer impedance increases approximately linearly, while the quadrupole transfer impedance saturate. This is because the flux lines of the quadrupole field mode are concentrated around the centre of the antenna loops, whereas the flux lines of the dipole mode are concentrated between the loops. This can be utilised to reduce the inter-loop coupling, without affecting the quadrupole transfer impedance too much. As a trade-off between inter-loop coupling and transfer impedance, the design value for the opening angle was set to 45°.

The longitudinal impedance of this "bare" pick-up, consisting of only the cavity and antenna loops was simulated (see Fig. 10). Several resonances are present. These can be split in two groups, depending on their origin. Strip-line type resonances in the antenna loops show up at regular intervals starting at about 150 MHz with a spacing of approximately 300 MHz. The cavity-related resonances are grouped in the high frequency part of the spectrum.

B The effect of metallic vanes

The quadrupole field component has four E-type symmetry planes. Metallic sheets (vanes) inserted in these positions does not change anything for the quadrupole field mode. However, such conducting boundaries are not compatible with lower-order field components, and the influence of these components are therefore reduced.

Simulations show that by introducing such vanes in the cavity outside the ceramic, the dipole transfer impedance (Fig. 8) is reduced by about 20% relative to the bare pick-up, while the quadrupole transfer impedance level is left unchanged (Fig. 9). More importantly, the vanes reduce the longitudinal impedance. The low-frequency inductance of the pick-up is reduced by a factor two and the peak value of the first resonance by almost the same amount (Fig. 11).

C The effect of symmetric loop terminations

Since the transformer end of the antennae have a ground connection, the opposite end of the loop should be left floating to avoid ground loop problems.

However, as mentioned above, the loop then forms a strip-line resonator that is excited by the beam. Close to the resonance, the loop current is enhanced and any imperfection leads to a strong parasitic common-mode signal on the output. The strip-line resonance also presents a large longitudinal impedance to the beam. To avoid this, the far end can be connected to ground via a suitably chosen resistor. The resistance should be chosen small enough to damp the resonance effectively, but large enough to keep the signal current from passing through ground. The design value was set to 200 Ω. The beneficial effect of the terminations on the longitudinal impedance can be seen in Fig. 12, where all the loop-related resonances are strongly damped. The simulated transfer impedances are unchanged, but measurement on a lab prototype showed a strong reduction in the parasitic common-mode signals.

D The effect of resistive coating

As mentioned above, the metallic layer on the ceramic gives a certain screening effect at high frequencies[5]. Simulations have been performed to find the optimum value of the resistivity of the layer.

In general, the cut-off frequency for a given coating resistivity was found to increase with the mode number of the field component. This is useful, since the longitudinal impedance is related to the lowest order (monopole) mode and is therefore reduced more efficiently than the transfer impedances corresponding to the dipole and quadrupole mode.

To minimise the longitudinal impedance, the coating resistivity should in principle be as low as possible. The lower limit is set by the desired bandwidth for the signals to be measured. A scan of coating resistivities showed that a surface resistance of about 3.5 Ω would give a cut-off around 25 MHz for the dipole signal and 30 MHz for the quadrupole signal. Measurements of the coupling impedance performed on a prototype pick-up with approximately this coating resistivity agreed well with the

simulations (see Figs. 15-16). Simulations of the longitudinal impedance gives a very small value, as shown in Fig. 13. Indeed the impedance was too small to be measured.

Unfortunately, when the layer is chosen to screen very efficiently, a relatively large part of the image current passes though the layer. This means that any imperfection in the roundness of the ceramic tube or the homogeneity of the layer will create parasitic dipole and quadrupole field modes through mode conversion. Therefore, the prototype pick-up with this low resistivity coating performed rather poorly in terms of common-mode rejection.

There are two solutions to this problem. Either one can tighten the tolerances on roundness and resistivity (which is expensive) or one can allow the beam to see a slightly larger impedance. Since the impedance levels involved are not high compared to the estimated total impedance of the PS machine, the second option was taken. Increasing the resistivity by about a factor 100 should sufficiently reduce the parasitic signals, while keeping the longitudinal impedance at a reasonable level (see Fig. 14). The transfer impedances are then practically unaffected by the coating in the frequency range up to 50 MHz (the simulated result is the same as in Fig. 8 and 9). Thus the coating surface resistance was fixed to about 300 Ω for the final model[6].

E Non-linear response to beam position

As well as the transfer impedance for the dipole and quadrupole modes, the transfer impedance for the sextupole mode was also extracted from the simulations (see Fig. 17). After the combination of the four loops signals in a hybrid circuit, the sextupole signal appears on the same output as the dipole signal, and therefore manifests itself as a nonlinearity in the position response. The sextupole coupling impedance, if it is known, can therefore be used to estimate and possibly correct for this nonlinearity.

V. CONCLUSIONS

Extensive simulations have been carried out to test a new design idea for a quadrupole pick-up. Several of the simulations have been compared to bench measurements on a prototype pick-up, all with very good agreement. This gives confidence in the simulated values that have not been verified experimentally. Through testing of various designs by simulations, it was possible to reduce the longitudinal impedance of the structure by two orders of magnitude, while maintaining the relevant pick-up transfer impedances as large as possible.

REFERENCES

[1] A. Chapman-Hatchett, A. Jansson, and D.J. Williams, in *Proceedings of 18th Particle Accelerator Conference* (New York, 1999), vol. 4, pp. 2223–2225.

[2] http://www.ansoft.com.

[3] A.W. Chao and M. Tigner, eds., *Handbook of Accelerator Physics and Engineering* (World Scientific, 1999), chap. 7.5.1.

[4] V. Vaccaro, *Coupling Impedance Measurements: An Improved Wire Method* (1994), INFN/TC-94/023.

[5] F. Caspers, G. Dome, C. Gonzalez, E. Jensen, E. Keil, M. Morvillo, F. Ruggerio, G. Schröder, B. Zotter, and M. D'Yachkov, in *Proceedings of 18th Particle Accelerator Conference* (New York, 1999), vol. 2, pp. 1408–1410.

[6] A. Jansson and D.J. Williams, *A New Optimized Design of Quadrupole Pick-up using Magnetic Coupling*, to be submitted to Nucl. Instr. Meth. in Phys. Res. A.

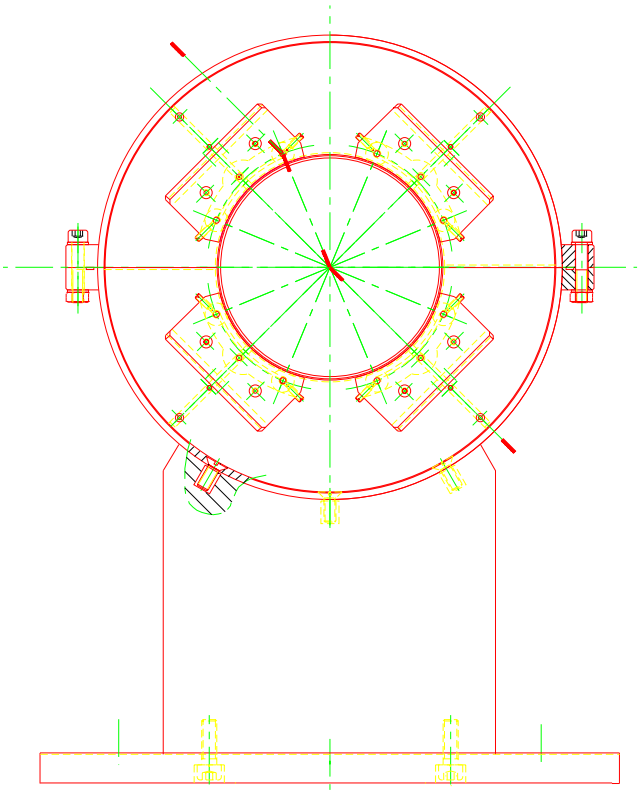

FIG. 1: CAD drawing of the pick-up, as seen along the beam path.

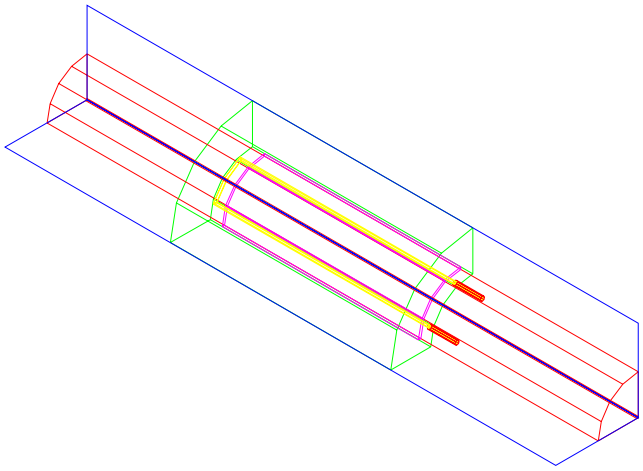

FIG. 2: HFSS model of the pick-up. Only one quarter of the pick-up was modelled, and symmetry boundaries were used to reduce the computing time.

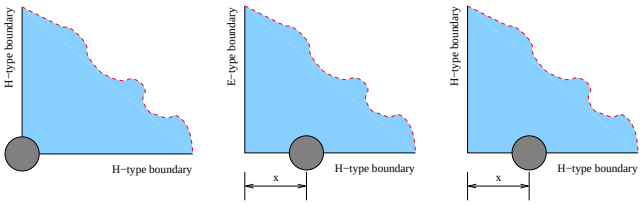

(a) Simulation of a coaxial wire for longitudinal impedance determination.

(b) Simulation of two parallel wires in anti-phase for position coupling impedance determination

(c) Simulation of two parallel wires in phase for quadrupole (beam width) coupling impedance determination

FIG. 3: Symmetry boundary settings for the different problems.

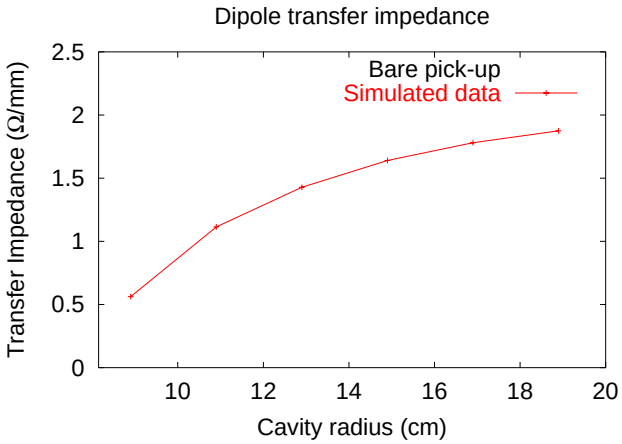

FIG. 4: Simulated average dipole transfer impedance in the pass-band of the "bare" pick-up as a function of the cavity radius. The loop opening angle was 45°, the beam pipe radius 7.25 cm and the antenna loops situated at 8.15 cm from the centre.

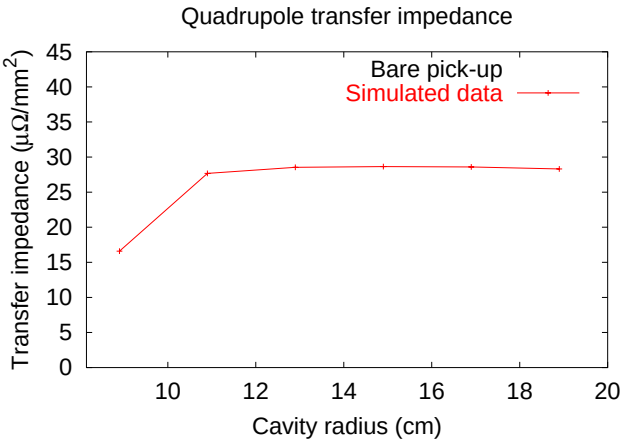

FIG. 5: Simulated average quadrupole transfer impedance in the pass-band of the "bare" pick-up as a function of the cavity radius. The loop opening angle was 45°, the beam pipe radius 7.25 cm and the antenna loops situated at 8.15 cm from the centre. Note that the value saturates faster than in the dipole case.

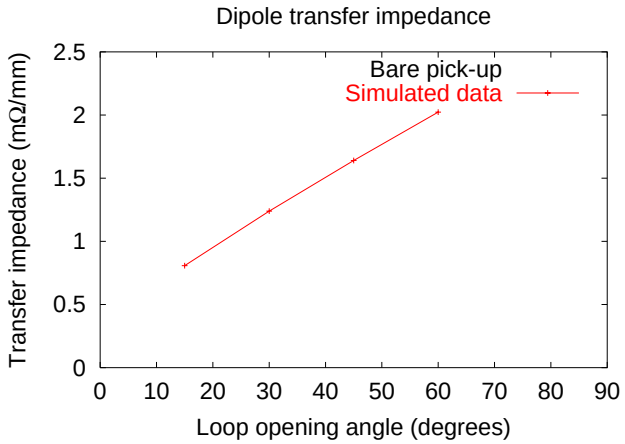

FIG. 6: Simulated average dipole transfer impedance in the pass-band of the "bare" pick-up as a function of the loop opening angle. The cavity radius was 15 cm and the pipe radius 7.25 cm

.

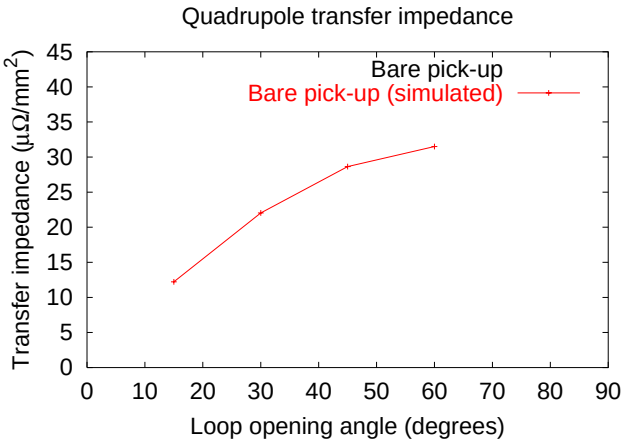

FIG. 7: Simulated average quadrupole transfer impedance in the pass-band of the "bare" pick-up as a function of the loop opening angle. The cavity radius was 15 cm and the pipe radius 7.25 cm. Note that, unlike in the dipole case, the value saturates.

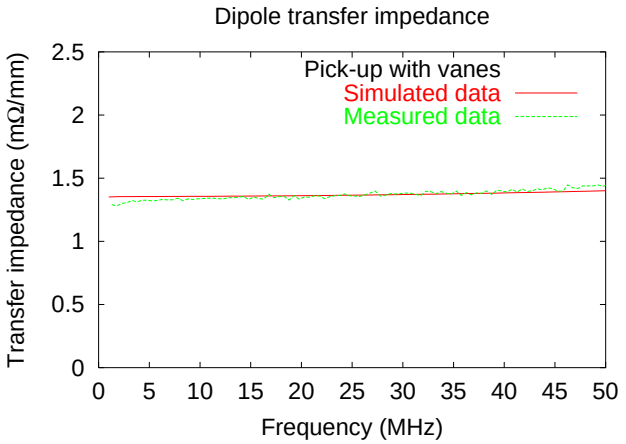

FIG. 8: Simulated and measured sensitivity to beam position for the pick-up with metallic vanes.

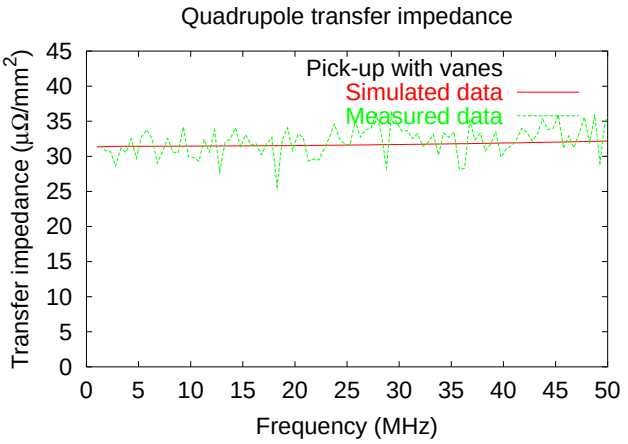

FIG. 9: Simulated and measured sensitivity to beam size (quadrupole moment) for the pick-up with metallic vanes. Because of the low signal levels, the measured data is strongly influenced by noise in the network analyser.

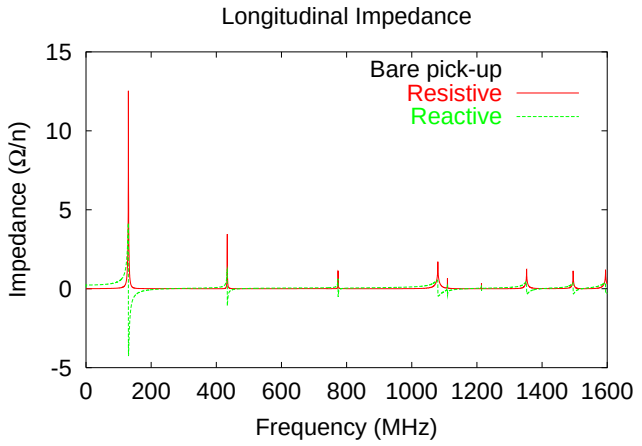

FIG. 10: Simulated longitudinal impedance of the "bare" pick-up. Note that the peak value at the resonances is only approximative since the formula for conversion of the s-parameter result into impedance is a perturbative result valid only for small impedances.

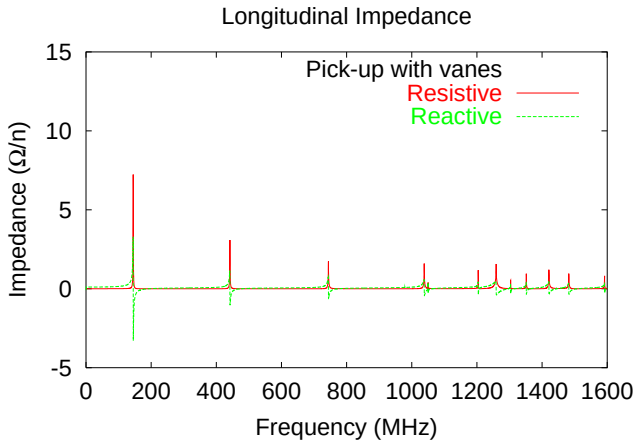

FIG. 11: Simulated longitudinal impedance of the pick-up with metallic vanes.

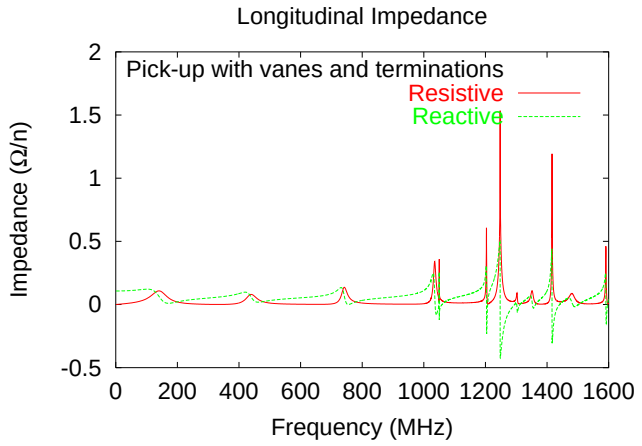

FIG. 12: Simulated longitudinal impedance of the pick-up with metallic vanes and 200 Ω loop terminations. The disappearance of the strip-line resonances was also observed experimentally. Note the change of scale relative to the previous graphs.

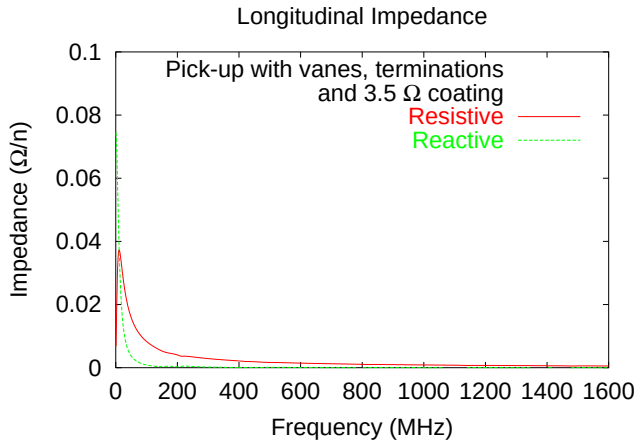

FIG. 13: Simulated longitudinal impedance for a pick-up with metallic vanes, 200 Ω loop terminations and a thin metal coating with resistivity 3.5 Ω. Note the change of scale relative to the previous graphs.

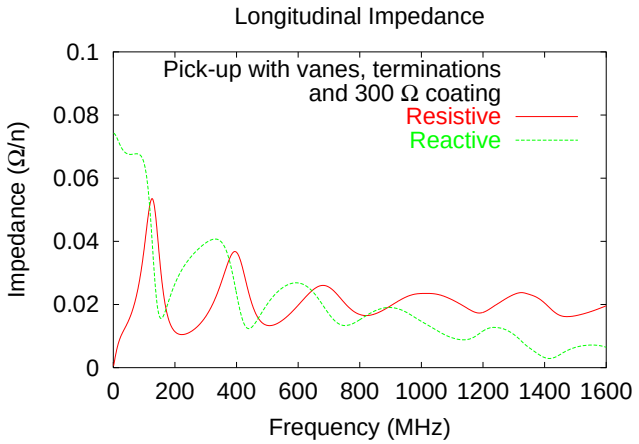

FIG. 14: Simulated longitudinal impedance for a pick-up with metallic vanes, 200 Ω loop terminations and a thin metal coating with resistivity 300 Ω.

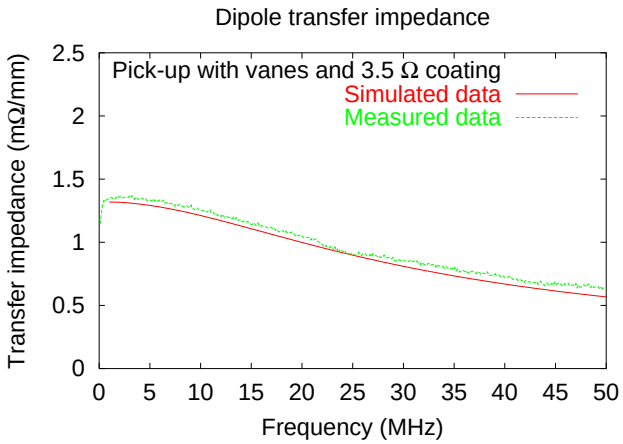

FIG. 15: Simulated and measured sensitivity to beam position for a pick-up with metallic vanes, 200 Ω loop terminations and a thin metal coating with resistivity 3.5 Ω.

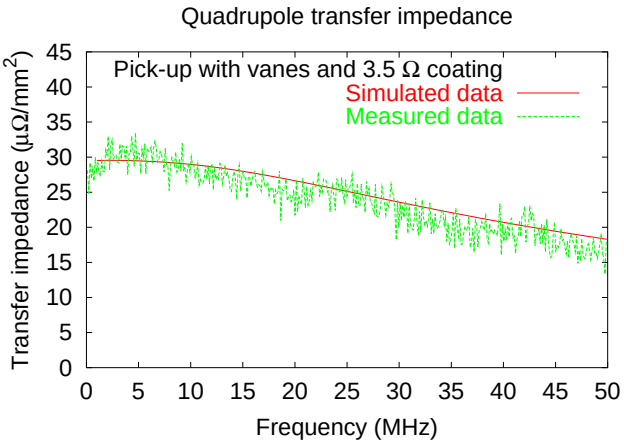

FIG. 16: Simulated and measured sensitivity to beam size (quadrupole moment) for a pick-up with metallic vanes, 200Ω loop terminations and a thin metal coating with resistivity 3.5 Ω.

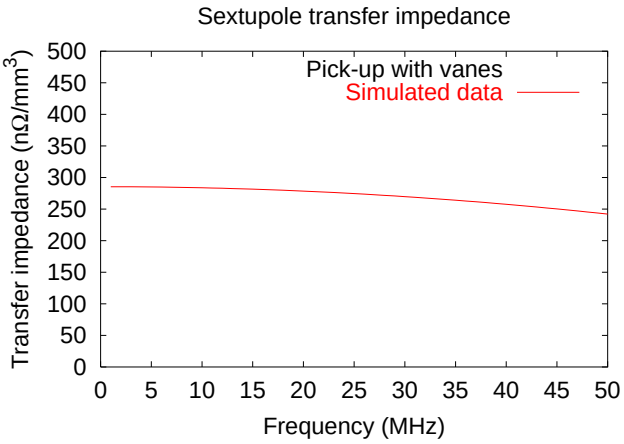

FIG. 17: Simulated sensitivity to the sextupole field moment (position non-linearity) for the pick-up with metallic vanes.